buildings

MDPI

Article

Experimental Investigation on the Strength and Microscopic Properties of Cement-Stabilized Aeolian Sand

Qiang Cui [1], Guang Liu [2,*], Zhenhua Zhang [2], Yiqiu Fang [2] and Xudong Gu [2]

[1] Institute of Transmission and Transformation Engineering, China Electric Power Research Institute, Beijing 102401, China
[2] School of Civil Engineering, Hefei University of Technology, Hefei 230009, China
* Correspondence: guang_liu@hfut.edu.cn

Abstract: Aeolian sand widely exists in the desert of western China. The reinforcement of aeolian sand is of considerable significance to the construction of transmission lines in the desert. In order to study the impact of different cement contents and moisture content on the performance of the cement-stabilized aeolian sand, 18 types of samples of aeolian sand with different water and cement contents were prepared. The confined and unconfined compression tests of the aeolian sand samples were conducted on the TSZ series automatic triaxial instrument. The microscopic observation methods and macroscopic strength tests were adopted to understand the cement-stabilized mechanism. The results of the triaxial test manifest that both the moisture content and the cement content affect the stress-strain behavior of the cement-stabilized aeolian sand. The cement-stabilized effect on aeolian sand can be estimated by the degree of hydration reaction. Microscopic test results show that as the cement content increases, the pores in the microstructure decrease, and some crystalline substances appear. The content of calcium silicate hydrate (C-S-H), which is one of the hydration products, is measured by the X-ray diffraction method. The results indicate that the solidification effect of cement is related to the C-S-H percentage. For 3% water content, the percentage of C-S-H goes up first with the increase of cement content and then gradually decreases at the cement content of 6%. When the water content goes up to 5% and 7%, it is found that the production of C-S-H gel increases with cement content.

Keywords: aeolian sand; cement content; microscopic test; sand stabilization; cement-stabilized sand; compression test

check for updates

Citation: Cui, Q.; Liu, G.; Zhang, Z.; Fang, Y.; Gu, X. Experimental Investigation on the Strength and Microscopic Properties of Cement-Stabilized Aeolian Sand. *Buildings* **2023**, *13*, 395. https://doi.org/10.3390/buildings13020395

Academic Editor: Moncef L. Nehdi

Received: 18 December 2022
Revised: 15 January 2023
Accepted: 19 January 2023
Published: 1 February 2023

Copyright: © 2023 by the authors. Licensee MDPI, Basel, Switzerland. This article is an open access article distributed under the terms and conditions of the Creative Commons Attribution (CC BY) license (https://creativecommons.org/licenses/by/4.0/).

1. Introduction

Due to the uneven distribution of hydropower, thermal power, and wind power in space, many countries need to build long-distance power transmission lines. Therefore, there will be many overhead transmission lines that need to cross the deserts, such as Zhundong-Southern Anhui (1100 kV), Yili-Kucha (1100 kV), and Bachu-Hetian (750 kV) ultra-high voltage transmission lines in China. The erection of these transmission lines involves reinforcing an aeolian sand foundation because aeolian sand widely exists in the desert of western China.

Aeolian sands consist of loose sediments formed by erosion, transportation, and deposition under weathering conditions in arid deserts. Some direct shear tests have shown that the cohesion parameter of aeolian sands is equal to zero, and the internal friction angles vary between 39 degrees and 42 degrees [1–3]. Therefore, the pull-out bearing capacity of the foundation of aeolian sand is usually challenging to meet in design requirements [4]. Especially in drought areas with sparse vegetation, surface grains of sand near tower foundations are easily blown away due to wind erosion, resulting in the reduction of the foundation burial depth. This loss of surface sand will significantly weaken the uplift bearing capacity of the foundations. Therefore, developing an effective

and feasible stabilized method for aeolian sands to improve the uplift bearing capacity of the foundations is one of the urgent technical problems that needs to be addressed in power transmission and transformation projects in desert areas.

The stabilization of aeolian sand is mainly carried out from three aspects: engineering methods, biological methods, and chemical methods. The engineering method generally paves geogrid, geotextile [5], fine metal wire mesh [6], nylon mesh [7], fibers and organic polymer [8], and other materials on the surface of aeolian sand. The primary purpose of the stabilization is to prevent the flow of sand particles and inhibit wind erosion on the ground. The biological approach is to plant vegetation or place microorganisms in the desert according to the actual situation. In order to investigate the stabilization effect of plant roots, the dynamic behavior of clay reinforced using wires has been examined by direct shear tests and Plaxis 2D simulation [9]. The biological method effectively suppresses erosion of the desert and improves the ecological environment of the desert by designing an effective plant protection system and structure.

The chemical method is commonly used in the practice of aeolian sand reinforcement. It mainly adds additives to improve the cohesion of aeolian sands [9–11]. The typical chemical additives can be cement, lime, fly ash, liquid polymer, and calcium carbide residue. A large number of laboratory tests on aeolian sand stabilization using bitumen admixtures as additives were performed in regions such as Saudi Arabia three decades ago [12–14]. Based on this research, many scholars have attempted different curing agents to reinforce sand, for instance, cement [11,15–19], bentonite, and lime [20]. Microscopic analysis shows that adding zeolite to cemented sand can reduce the porosity of its microstructure, which causes the strength to increase [21].

Recent research results show that the strength of the cemented binary mixtures increases with water content and the water-to-cement ratio until a threshold value is reached and then decreases with further increase in water content and the water-to-cement ratio. In [22,23], the authors investigated the influence of water content and the water-cement ratio on strength with laboratory compressive tests on specimens with the given density and void ratio. Jumassultan et al. [24] conducted comprehensive laboratory work to assess the effect of the cyclic freeze-thaw action on the strength and durability of calcium sulfoaluminate cement-treated sand. Research indicates that zeolite can be used along with cement as a stabilizer to enhance the mechanical behavior of the soils [25]. The in situ sand and soil stabilization by cement has a wide range of applications in practical engineering (including highway and road construction, transmission line tower foundation, and foundation reinforcement in civil engineering) due to its better economic and environmental benefits [26].

The purpose of this research is to explore the micro-mechanism of the interaction between additives and aeolian sand from a microscopic perspective in order to further improve the reinforcement effect in engineering. This study conducted triaxial tests on the different aeolian sand samples to understand the reinforcement effect of varying moisture content and cement content. We then adopted microscope observation, elemental energy spectrum analysis, and X-ray diffraction to investigate the solidification mechanism of cement-reinforced aeolian sand on a microscopic scale. Through the combination of microscopic observation means and strength tests, this study reveals the specific mechanism of cement-stabilized aeolian sands in depth, which provides an important reference for foundation reinforcement treatment in desert areas.

2. Samples and Methods

2.1. Sampling Site

Figure 1 shows the sampling locations of the aeolian sand samples used in this study. The sampling site at 77°46′58.30″ east longitude and 39°36′22.24″ north latitude is at the bottom of a typical tower in Bachu County, Kashi City, Xinjiang, China. This area, with an altitude of 1136 m, is located in the hinterland of the Taklimakan Desert. The climate here is arid, with an annual rainfall of no more than 100 mm and annual evaporation of

2500–3000 mm. There are frequent sandstorms in this area. Mobile dunes account for more than 80%, with an average wind speed of 5.9 m/s. In order to facilitate the test, the aeolian sand at this place was first bagged in storage bags with a volume of 1.5 m × 1.5 m × 1.5 m. The physical and mechanical properties of the aeolian sand samples were tested after being transported to the State Grid Corporation Geotechnical Engineering Key Laboratory Hall.



Figure 1. The sampling site of aeolian sand.

The main mineral composition of the aeolian sand can be obtained from X-ray diffraction tests and SEM tests. From the test results from X-ray diffraction, it can be seen that the aeolian sand is mainly composed of quartz, feldspar, and calcite, of which quartz accounts for up to 77%. The total content of the three minerals exceeds more than 90% of the total mass, and minerals such as mica and kaolinite only account for about 9%. The aeolian sand appears to be in the form of loose particles, and there is basically no adhesion between the particles.

Before we use cement to reinforce the aeolian sand, it is necessary to figure out the water content of the aeolian sand on site. According to the alcohol burning method recommended in the Geotechnical Test Regulations of China (SL237-1999), the natural water content of shallow aeolian sand within 2 m was measured, as shown in Figure 2. The test and analysis results show that the in situ natural density of the aeolian sand sample was 1.43 g/cm^3. The on-site density and moisture content tests are shown in Figure 2.



(**a**) (**b**)

Figure 2. On-site density and moisture content tests. (**a**) On-site density test; (**b**) Field test equipment for water content.

Figure 3 indicates that the moisture content of the shallow aeolian sand sample increases linearly with the increase of the sampling depth. The result shows that the moisture content of aeolian sand changes within 2%.

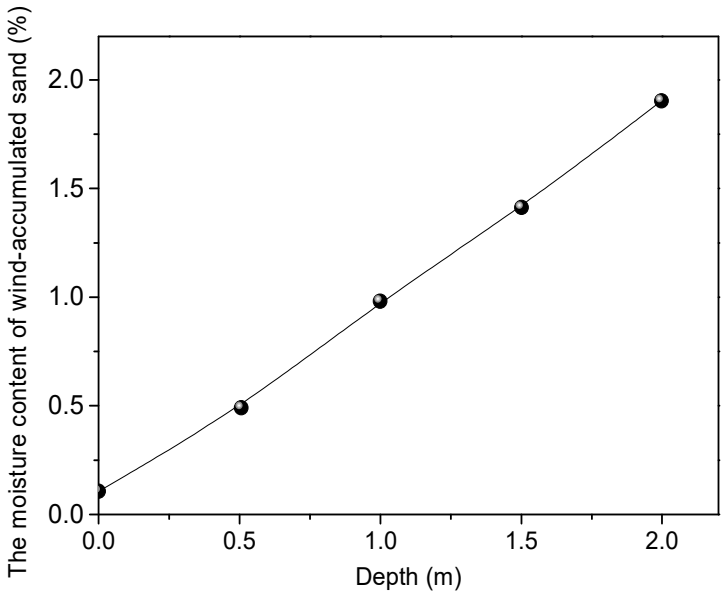


Figure 3. Variation curve of water content with depth for shallow aeolian sand.

2.2. Strength Test Preparation

Field test tests show that the water content of shallow aeolian sand in the Taklimakan Desert in southern Xinjiang is generally low, within about 3%. Related research shows that the natural moisture content of desert regions in China varies from 2% to 4% [27]. In order to study the compressive strength of cement-stabilized aeolian sand, this test prepared 18 types of samples with a water content of 3%, 5%, and 7%, and cement content of 4%, 6%, and 8%. The specific information for the 18 types of samples is given in Table 1. The cement used in this study of aeolian sand stabilization is ordinary Portland cement.

Table 1. Water contents and cement contents of test samples.

No. [a]	Moisture Content (%)	Cement Content (%)
3-4-1	3	4
3-4-2		
3-6-1		6
3-6-2		
3-8-1		8
3-8-2		
5-4-1	5	4
5-4-2		
5-6-1		6
5-6-2		
5-8-1		8
5-8-2		
7-4-1	7	4
7-4-2		
7-6-1		6
7-6-2		
7-8-1		8
7-8-2		

[a] The first value in the label represents the moisture content (%), the second value represents the cement content (%), and the third value represents the test group number.

The sample preparation process follows the steps below.

(1) A standard sieve with an aperture of 2 mm is used to sieve the aeolian sand to obtain fine particles.
(2) According to the water content and cement contents shown in Table 1, a certain amount of water and Portland cement were added to the air-dried aeolian sand. Then we stirred the aeolian sand evenly and sealed it with plastic wrap for one day.
(3) We sprayed some water on the inner wall of the triaxial sample maker and attached the plastic wrap to the inner wall of the sample maker.
(4) The sample was compacted in 3 layers according to the sample height. During the compaction process, all layers of soil had equal quality. After each layer was compacted to the required height, we shaved the surface and then added another layer of soil. This process continued until the last layer was compacted. Subsequently, both ends of the sample were flattened. These samples were taken out after one day of natural hardening in the compaction equipment. These specimens were placed in the laboratory for 14 days prior to the triaxial compressive tests. The formed triaxial test sample has a diameter of 31.9 cm and a height of 8 cm, as shown in Figure 4.



(**a**) w_w = 3%, w_c = 4%, Group 1



(**b**) w_w = 3%, w_c = 6%, Group 2



(**c**) w_w = 5%, w_c = 6%, Group 1



(**d**) w_w = 5%, w_c = 8%, Group 2

Figure 4. *Cont.*



(**e**) w_w = 7%, w_c = 4%



(**f**) w_w = 7%, w_c = 8%, Group 2

Figure 4. Triaxial compressive test samples with different water contents and cement contents.

The test samples were prepared according to a uniform method to ensure that their size, shape, and compaction degree were consistent. The triaxial compressive strength test of the aeolian sand samples was conducted on the TSZ series automatic triaxial instrument (see Figure 5). Before the test, the prepared aeolian sand samples were wrapped with a geotechnical latex mold and installed in the corresponding position of the sample in the confining chamber. Next, the confining pressure was set to the required value. The triaxial undrained and unconsolidated compression test was performed using an axial loading speed of 0.6 mm/min.



Figure 5. TSZ series automatic triaxial instrument.

2.3. Microscopic Test Methods

The macro-mechanical performance of the material is strongly related to its microstructure characteristics [28–31]. In this section, we will analyze the micro-mechanism of cement-reinforced aeolian sand from the perspectives of the microstructure, element, and mineral composition. In order to study the changes in the microstructure and composition of the cement-stabilized aeolian sand, SEM observations and elemental energy spectrum tests were conducted on the 18 types of samples shown in Table 1. The SEM observation tests of

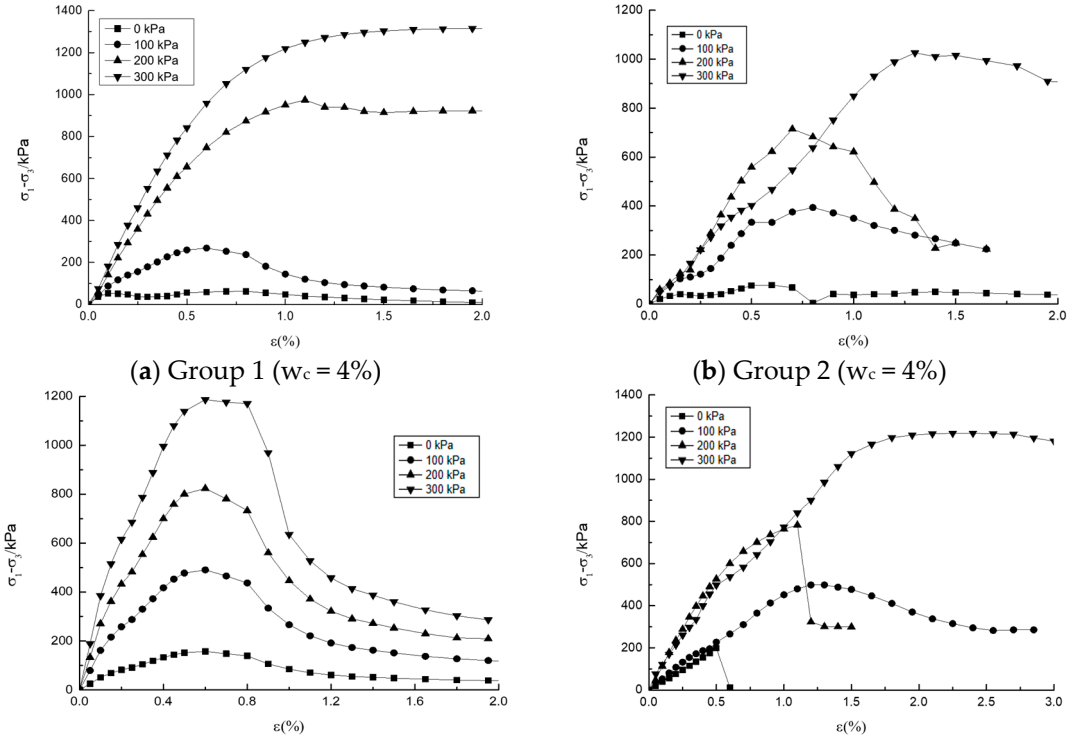
aeolian sand samples were performed on the field emission electron microscope (SU8020). The specific test procedures are described in the following paragraph.

A small piece of sample block, with a diameter no greater than 10 mm, was taken from the prepared sample. A flat, fresh section was chosen for the microscopic observation. The conductive glue was adopted to stick the sample bulk to the sample pile, which ensured the flat, fresh section had full contact with the upper surface of the sample pile. The dust attached to the sample needs to be removed before observation. It is better to select a relatively flat surface to observe under the scanning electron microscope. After the observation of the morphological characteristics of the mineral aggregates, we chose an appropriate sample surface for the energy spectrum point test.

3. Results and Discussion

3.1. Influence of Cement Contents on the Compressive Strength

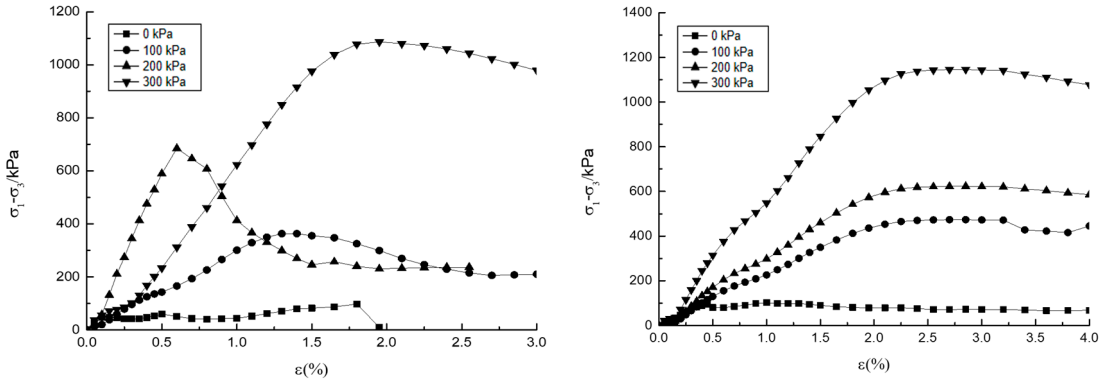
Even under the same moisture content and cement content conditions, the strengths of the aeolian sand samples are different. In order to fully consider the strength variability of aeolian sand samples, two groups of samples were tested for both water and cement content. The water content in Figure 6 is 3%, and the cement content is 4%, 6%, and 8%. For each cement and water ratio, Figure 6 shows the stress-strain curves under different confining pressures. Many factors contribute to the strength dispersion of cement-stabilized aeolian sands, including moisture content, cement content, microstructure, pore distribution, etc. Group 1 and Group 2 samples only have the same moisture content and cement content, and it is difficult to control other strength-related factors to be the same. Therefore, it is also understandable that there is a difference in the strength of the two groups of specimens. Generally speaking, for cement-stabilized aeolian sands with certain cement and water contents, their peak strength and residual strength basically increase with the increase of confining pressure. Nevertheless, the relation between strength and cement content seems complicated under a certain confining pressure and water content.



(**a**) Group 1 (w_c = 4%) (**b**) Group 2 (w_c = 4%)

(**c**) Group 1 (w_c = 6%) (**d**) Group 2 (w_c = 6%)

Figure 6. *Cont.*



(**e**) Group 1 (w_c = 8%) (**f**) Group 2 (w_c = 8%)

Figure 6. Stress-strain curves of cement-stabilized aeolian sands under different confining pressures with a water content of 3%.

To study the effect of cement content on the strength of cement-stabilized aeolian sand, Figure 7 shows the peak strength at two confining pressures of 0 kPa and 100 kPa. The peak strength of cement-stabilized aeolian sand is affected by both the cement content and the water content. When the water content is low, the peak strength first increases with the cement content and then shows a downward trend. The reason may be that the low water content is not enough to support a large amount of cement for hydration reaction. The cement fails to hydrate to form an adhesive material, which fully limits the reinforcement effect. There are several tests in which the strength of the cement-stabilized aeolian sand decreases with increasing the cement content. These phenomena occur mainly in the case of low moisture content and high cement content. In this case, the cement absorbs a large amount of water. Insufficient water content leads to an incomplete hydration reaction of cement, which produces little C-S-H gel. Therefore, at a low water-cement ratio, i.e., low water content and high cement content, the cement-stabilization effect is not obvious. When the water content is sufficient, cement is more likely to undergo a complete hydration reaction. In this case, the peak strength of aeolian sand tends to increase as the cement content increases, which is consistent with the results of trials conducted by other researchers [16]. When the confining pressure goes up, the reinforcement effect of the cement is more prominent (see Figures 7 and 8).

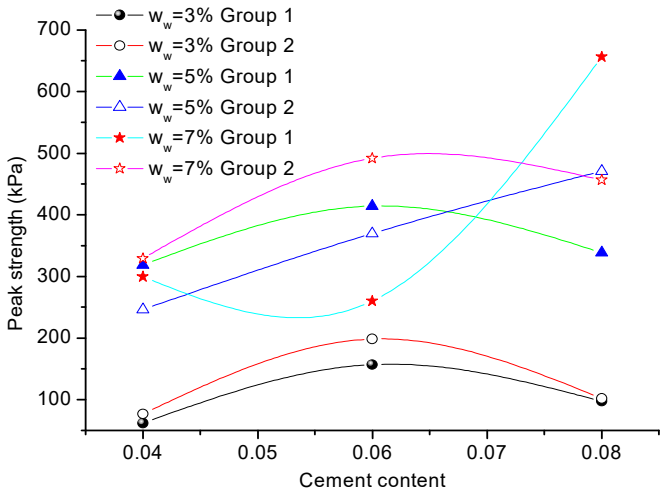


Figure 7. Variation of peak strength with cement contents under unconfined state.

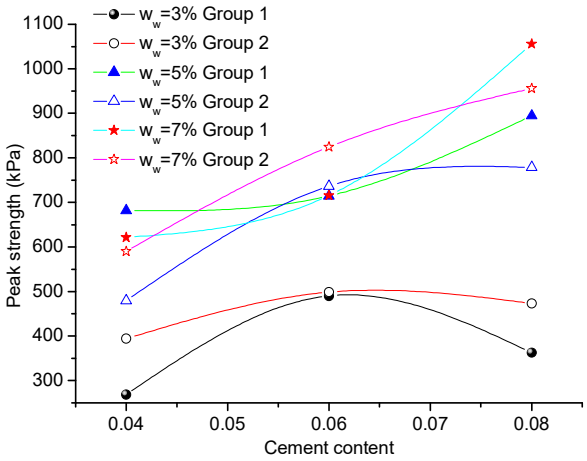


Figure 8. Variation of peak strength with cement contents under confining pressure of 100 kPa.

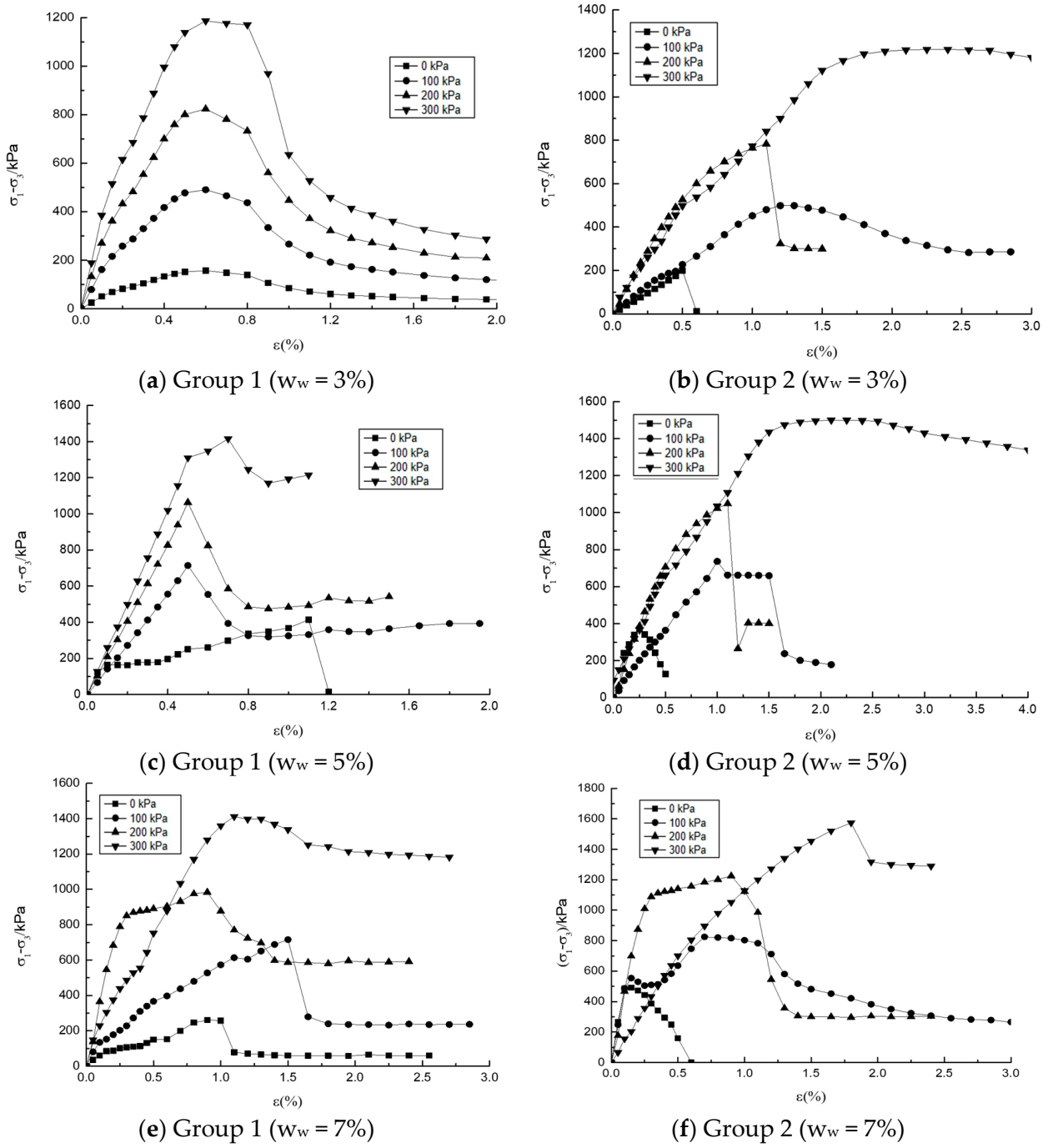
Table 2 shows the internal friction angle and cohesion of cement-stabilized aeolian sand samples with different water and cement contents. As seen in Table 2, the cohesion of the cement-stabilized aeolian sand sample increases with the increase of cement content except for the sample with 3% water content. The effect of cement content on the internal friction angle is not apparent. It can be concluded that the difference in internal friction angle and cohesive force is primarily caused by the different bonding degrees of the aeolian sand particles. Under a low water content (3% water content), the degree of bonding of aeolian sand and cement is weak. The confining pressure in the triaxial test can effectively compact the aeolian sand sample, which effectively improves its cohesion.

Table 2. Cohesion and internal friction angle of cement-stabilized aeolian sand with different water and cement contents.

Water Content (%)	Cement Content (%)	Internal Friction Angle (°)	Cohesion (kPa)
3	4	31.19	22.23
	6	33.21	40.61
	8	32.43	22.61
5	4	35.27	77.65
	6	32.72	103.75
	8	33.81	117.78
7	4	31.45	82.71
	6	34.61	126.44
	8	36.74	164.53

3.2. Influence of Water Contents on the Compressive Strength

In this section, we fixed the cement content of the specimens and investigated the effect of water content in the cement-stabilized aeolian sand on its strength. The same test procedure was used to perform triaxial tests for aeolian sand tests with different water contents. For each type of specimen in the test, the confining pressures are 0, 100, 200, and 300 kPa, respectively. The cement content in this section was fixed at 6%, and the water content was 3%, 5%, and 7%, respectively. As shown in Figure 9, the confining pressure effect is significant for the strength increase of the cement-stabilized aeolian sand specimens. However, the effect of water content on the strength of the cement-stabilized aeolian sand seems to be less obvious (see Figure 9).



(**a**) Group 1 (w_w = 3%) (**b**) Group 2 (w_w = 3%)

(**c**) Group 1 (w_w = 5%) (**d**) Group 2 (w_w = 5%)

(**e**) Group 1 (w_w = 7%) (**f**) Group 2 (w_w = 7%)

Figure 9. Stress-strain curves of cement-stabilized aeolian sands under different confining pressures and cement content of 6%.

To explain the effect of water content more clearly, the curve of the peak strength of the cement-stabilized aeolian sand with water content is plotted in Figure 10. The peak strengths in the triaxial compression test of the cement-stabilized aeolian sand increase overall with increasing water content at the given cement contents of 4%, 6%, and 8%. It can be seen in Figure 10 that this strength enhancement of the cement-stabilized aeolian sand is significant at a higher cement content and water content. At low cement content, e.g., 4%, a large amount of water can also cause a reduction in the compressive strength of the cement-stabilized aeolian sand. Therefore, the high moisture content will conversely reduce the strength of the cement-stabilized aeolian. The water content should be determined according to the cement content in order to be able to hydrate fully with the cement.

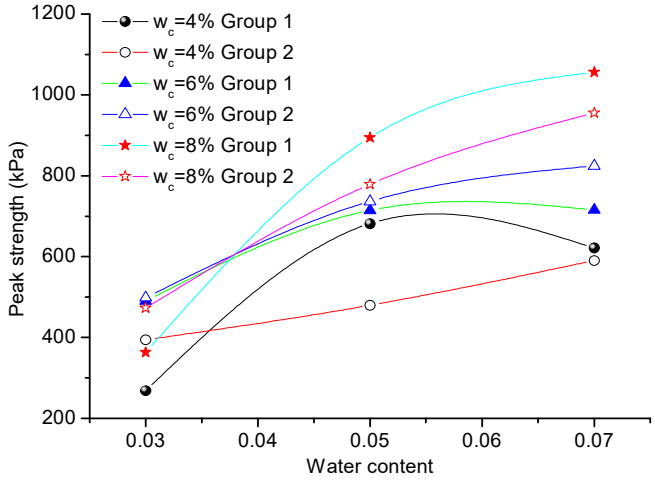


Figure 10. Variation of peak strength with water contents under confining pressure of 100 kPa.

3.3. Microstructures of Cement-Stabilized Aeolian Sand

As mentioned above, both the moisture and cement contents affect the macro-mechanical performance of cement-stabilized aeolian sand. We adopted the aeolian sand samples with a moisture content of 3% and different cement contents to perform the microscopic observation in this section. The microscopic observations used in this section include SEM observation, X-ray diffraction, and energy spectrum analysis.

The original aeolian sand sample structure is loose, with discrete sand grains and large voids (see Figure 4). After it is mixed with 4% cement, its surface structure is rough, with a large amount of cement grain agglomerates on the surface. For each cement content sample, we took two pictures with 50 times and 5000 times magnification. Figure 11 shows very clearly the microstructure of cement-stabilized aeolian sand with different cement contents, which is very helpful in understanding the cement-stabilized mechanism at the microscopic level. It can be seen from Figure 11 that some of the voids are filled with cement. The samples in Figure 11 remain at the same moisture content of 3%. Most of the attachments on the sand grains are needle-like crystals, and a small number of attachments are plate-like crystals. When the cement content reaches 6%, the surface structure becomes smoother, showing an apparent surface cementation phase. As the voids are further filled, fewer voids can be observed. A layer of fine crystals forms on the surface of the sand. The cement particles are relatively dense, and a large number of needle-like and plate-like crystals are attached in a network-like distribution. For the sample with 8% cement, its microstructure surface is rough, and a large number of lamellar crystals are attached to the surface. The microstructure image shows that large voids are filled, and only tiny voids can be seen. The microstructure density of the aeolian sand sample surface is further improved with the increase of the cement content. The number and distribution area of voids are reduced with the rise of crystal attachments on the surface. Overall, the microstructure of cement-stabilized aeolian sand seems to become denser as the cement content increases, which may be the reason why cement can reinforce aeolian sands.

Compared with the pure aeolian sand sample, the elemental composition of the sand sample mixed with cement has not changed much. After the aeolian sand is mixed with cement, the oxygen content does not change much, but the calcium content increases significantly (see Figure 12). Although the calcium content increased after adding cement, there was no clear relationship between this increase and the cement content. In general, the content of silicon, sodium, and aluminum decreased somewhat. It should be noted that the energy spectrum analysis can only reflect the element composition at the measurement point. Due to the uneven mixture of cement and aeolian sand, the element content in the sample may vary significantly.

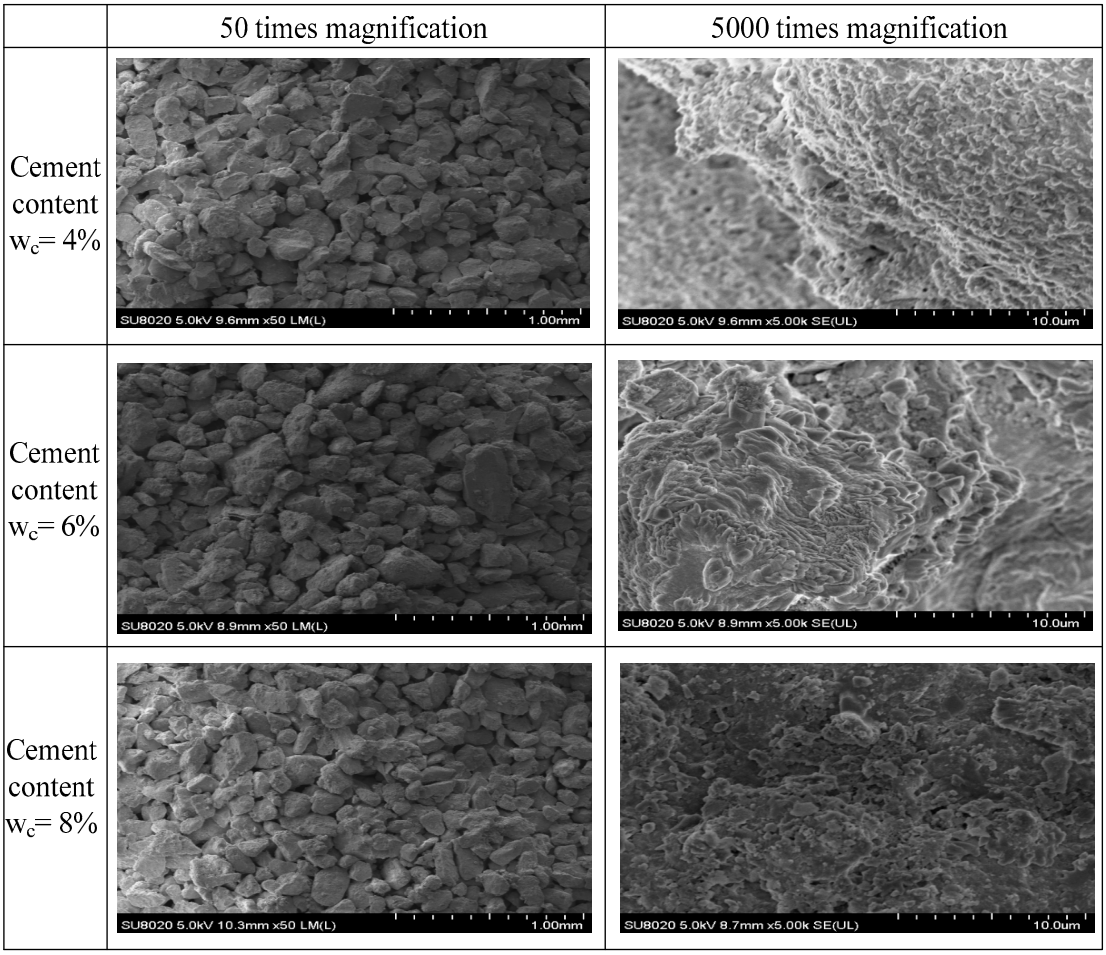
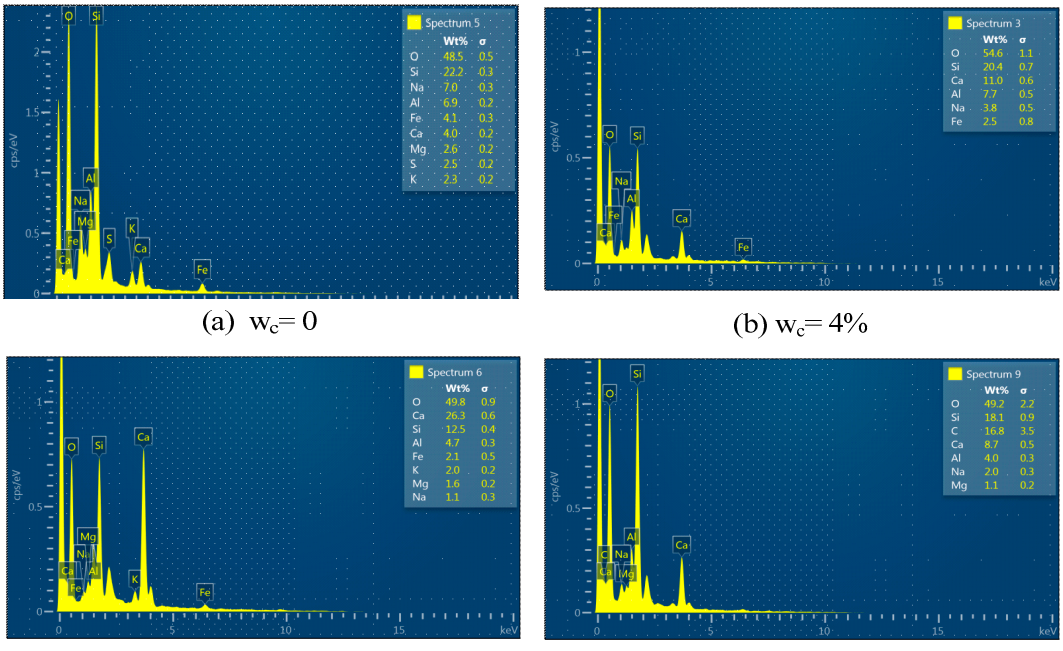


Figure 11. Microstructure images of cement-stabilized aeolian sand with different cement contents.



(a) w_c= 0 (b) w_c= 4%

(c) w_c= 6% (d) w_c= 8%

Figure 12. Element Spectrum of the cement-stabilized aeolian sand with different cement contents.

Using the X-ray diffraction test, we can obtain the mineral composition and percentage content of cement-solidified aeolian sand samples with different ratios, as shown in Figure 13. It can be seen that the pure aeolian sand sample is mainly composed of quartz, feldspar, calcite, and kaolinite. The kaolinite and albite in the aeolian sand have a complex physicochemical effect with the cement, which generates three hydration products, including calcium hydroxide, calcium silicate hydrate (C-S-H), and ettringite. Among these hydration products, C-S-H is a gel with good adsorption and cementing characteristics. This physicochemical effect may reveal the micro-mechanism to strengthen aeolian sand with cement. In other words, the hydration reaction between the cement and minerals in aeolian sand converts aeolian sand from discrete grains to cemented grains. This change improves the carrying capacity of aeolian sand from the microstructure level.

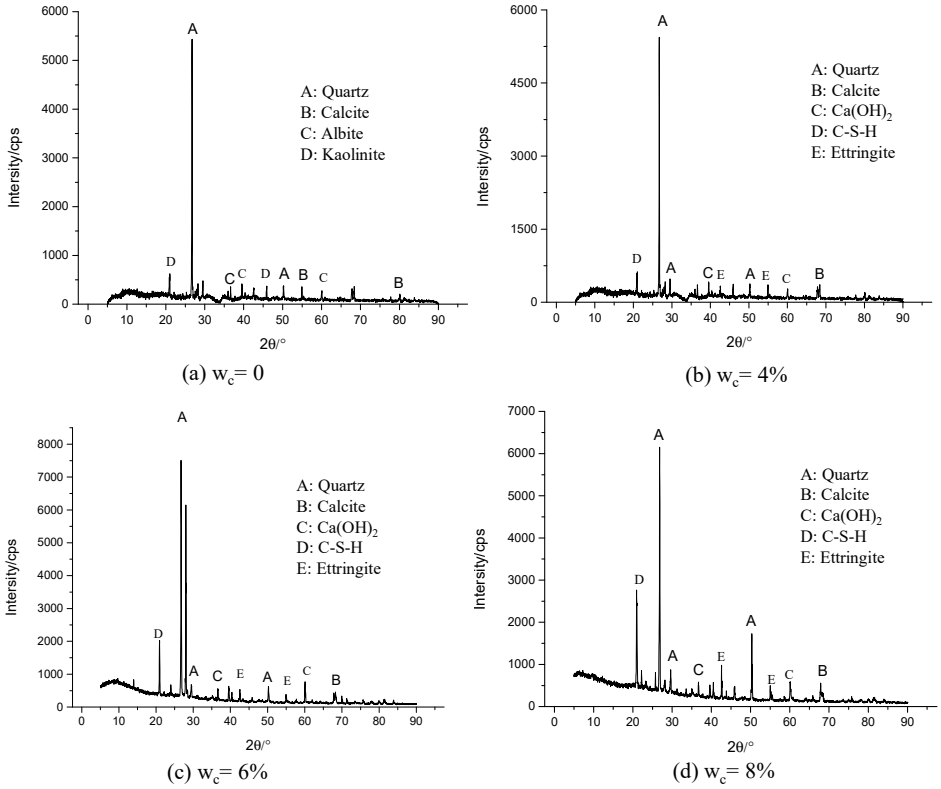


Figure 13. X-ray diffraction patterns of the cement-stabilized aeolian sand with different cement contents.

As mentioned above, both water content and cement content can affect the stress-strain curves of cement-stabilized aeolian sand. To investigate the degree of hydration, hydration product C-H-S is measured by the X-ray diffraction method. At a low cement content (4–6%), our results show that the strength of cement-stabilized aeolian sand increases and then decreases with water content. This variation trend of peak strength is consistent with the results given by [23]. At a high cement content (8%), there is a trend of increasing strength of cement-stabilized aeolian sand with increasing water content, and no obvious peak point is found in the range of 7% water content. The peak point of strength may arise after 7% water content. Since both water content and cement content affect the strength, the relationship between the water-cement ratio and strength has been specifically investigated in a large number of reports [23,32,33]. Figure 14 illustrates the variation of hydration product C-H-S with cement contents. For 3% water content, the percentage of C-S-H goes up first with the increase of cement content and then gradually decreases at the cement content of 6%. However, for high water content (5% and 7%), the production of the C-S-H gel increases consistently with cement content. It does not show a significant peak, which is generally in accordance with the trend of strength with cement content.

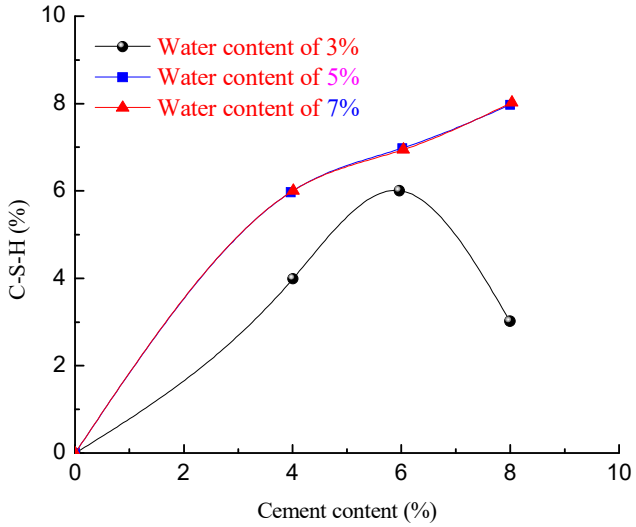


Figure 14. Variation curves of C-S-H and cement contents under different water contents.

Our microscopic analysis identified the presence of the cementitious products C-S-H, which was also found in previous research [34]. The results show that the cement content of 6% seems to achieve a good reinforcement effect for the samples with a water content of 3%. For the samples with a water content of 5% and 7%, the variation of C-S-H percentage shows similar monotone increasing curves, as shown in Figure 14. These characteristics are consistent with the aforementioned trends of the peak strength, which implies that the solidification effect of cement is related to the percentage of C-S-H.

4. Discussions

The reinforcement of aeolian sand is an essential foundation for constructing transmission lines in the desert. This research examines the solidified mechanism of cement-stabilized aeolian sand from a microscopic view. The mechanical strength of cement-solidified aeolian sand was studied through triaxial tests with different water content and cement content. Several cement- and water-content combinations were designed for this study, and strength tests for 18 types of cement-stabilized aeolian sand samples were conducted.

It should be noted that the actual cement and water content may vary in a wide range in different regions. The cement and moisture content used in the tests in this research mainly refer to the relevant engineering experience of aeolian sand stabilization in Xinjiang, China. The conclusions obtained in this study apply to specimens with moisture content and cement content in this interval. When the water and cement content exceed this interval, additional tests are needed to verify the validity of the conclusions. In addition, the stabilization method of aeolian sands used in this study is relatively simple, mainly through the addition of cement. In the next word, multiple stabilization methods, including engineering, biological, and chemical methods, should be tried to jointly reinforce the aeolian sands.

5. Conclusions

This study investigates the solidified mechanism of cement-stabilized aeolian sand by combining microscopic analysis methods and macroscopic strength tests. The main conclusions are as follows:

When the cement content is fixed, the peak strength of cement-stabilized aeolian sand tends to increase in general as the moisture content changes. At a relatively low water content, i.e., 3%, the strength of cement-stabilized aeolian sand first increases with the cement content, followed by a slight downward trend with the increase of cement content. When the water content reaches 5% and 7%, the strength of cement-stabilized aeolian sand

is generally increased with the increase in cement content. The strength variation with cement contents reveals that the strength improvement of cement-stabilized aeolian sand depends on the degree of cement hydration.

Microscopic observation experiments show that the microstructure, element, and mineral composition of cement-stabilized aeolian sand display dissimilar features from those obtained from pure aeolian sand. The variation magnitude of the microstructure is related to the amount of cement and water added. With the increase in cement content, the number of pores in the microstructure decreases, and the crystalline material formed by the cement-hydration reaction increases. The element spectrum indicates that the main element composition of the cement-stabilized aeolian sand has no significant change compared with pure aeolian sand. The X-ray diffraction test manifests that the pure aeolian sand sample is mainly composed of quartz, feldspar, calcite, and kaolinite.

Author Contributions: Conceptualization, Writing and Supervision, Q.C., G.L. and Z.Z.; Formal analysis, Y.F. and X.G. All authors have read and agreed to the published version of the manuscript.

Funding: The financial support for the research project includes: Study on some environmental factors of the transmission line (No. GCB17201400162), the National Natural Science Foundation of China (Grant no. 52009024), the Fundamental Research Funds for the Central Universities (JZ2022HGTB0273, PA2021KCPY0031), and Innovation and entrepreneurship funds for returnees of Hefei, and they are gratefully acknowledged.

Data Availability Statement: Some or all data, models, or code that support the findings of this study are available from the corresponding author upon reasonable request.

Conflicts of Interest: The author declares that there is no conflict of interest.

References

1. Al-Sanad, H.; Ismael, N.; Nayfeh, A. Geotechnical properties of dune sands in Kuwait. *Eng. Geol.* **1993**, *34*, 45–52. [CrossRef]
2. Al-Taie, A.J.; Al-Shakarchi, Y.J.; Mohammed, A.A. Investigation of geotechnical specifications of sand dune soil: A case study around Baiji in Iraq. *IIUM Eng. J.* **2013**, *14*, 121–132. [CrossRef]
3. Padmakumar, G.; Srinivas, K.; Uday, K.; Iyer, K.; Pathak, P.; Keshava, S.; Singh, D. Characterization of aeolian sands from Indian desert. *Eng. Geol.* **2012**, *139*, 38–49. [CrossRef]
4. Elipe, M.G.; López-Querol, S. Aeolian sands: Characterization, options of improvement and possible employment in construction—The State-of-the-art. *Constr. Build. Mater.* **2014**, *73*, 728–739. [CrossRef]
5. Deb, K.; Konai, S. Bearing capacity of geotextile-reinforced sand with varying fine fraction. *Geomech. Eng.* **2014**, *6*, 33–45. [CrossRef]
6. Al-Abdullah, S.F. An approach in improving the properties of sand dunes. *J. Eng.* **2006**, *13*, 930–939.
7. Wang, W.F.; Fan, J.T.; Zhang, W.M.; Qu, J.J.; Lin, B. Research on the Protective Effect of Nylon Mesh Fence on the Top of Dunhuang Mogao Grottoes. *Chin. Desert* **2005**, *25*, 640–648.
8. Liu, J.; Bai, Y.; Song, Z.; Kanungo, D.P.; Wang, Y.; Bu, F.; Chen, Z.; Shi, X. Stabilization of sand using different types of short fibers and organic polymer. *Constr. Build. Mater.* **2020**, *253*, 119164. [CrossRef]
9. Chenari, R.J.; Pishkhani, S.S.; Fard, M.K.; Sosahab, J.S. Experimental and numerical investigation of dynamic properties of soil stabilized by young Vetiver. *Ital. Geotech. J.* **2018**, *52*, 49–58.
10. Chenari, R.J.; Fatahi, B.; Ghorbani, A.; Alamoti, M.N. Evaluation of strength properties of cement stabilized sand mixed with EPS beads and fly ash. *Geomech. Eng.* **2018**, *14*, 533–544.
11. Pongsivasathit, S.; Horpibulsuk, S.; Piyaphipat, S. Assessment of mechanical properties of cement stabilized soils. *Case Stud. Constr. Mater.* **2019**, *11*, e00301. [CrossRef]
12. Akili, W.; Monismith, C. Permanent deformation characteristics of cement-emulsion stabilized sand. In *Proceedings Association of Asphalt Paving Technologists Technical Sessions*; Association of Asphalt Paving Technologists: Lino Lakes, MN, USA, 1978; Volume 47, pp. 281–301.
13. Al-Abdulwahhab, H.; Bayomy, F.; Al-Halhouli, A. Evaluation of Emulsified, Asphalt-Treated Sand for Low-Volume Roads and Road Bases. *Transp. Res. Rec.* **1987**, *1106*, 71–80.
14. Wahhab, H.; Abduljauwad, S. A study of soil stabilization in the Eastern Province of Saudi Arabia. In Proceedings of the 11th International Road Federation World Meeting, Seoul, Republic of Korea, April 1989; Volume 3, pp. 117–120.
15. Shooshpasha, I.; Shirvani, R.A. Effect of cement stabilization on geotechnical properties of sandy soils. *Geomech. Eng.* **2015**, *8*, 17–31. [CrossRef]
16. Shalabi, F.I.; Mazher, J.; Khan, K.; Alsuliman, M.; Almustafa, I.; Mahmoud, W.; Alomran, N. Cement-stabilized waste sand as sustainable construction materials for foundations and highway roads. *Materials* **2019**, *12*, 600. [CrossRef] [PubMed]

17. Subramanian, S.; Khan, Q.; Ku, T. Effect of sand on the stiffness characteristics of cement-stabilized clay. *Constr. Build. Mater.* **2020**, *264*, 120192. [CrossRef]
18. Du, J.; Zheng, G.; Liu, B.; Jiang, N.-J.; Hu, J. Triaxial behavior of cement-stabilized organic matter–disseminated sand. *Acta Geotech.* **2021**, *16*, 211–220. [CrossRef]
19. Mola-Abasi, H.; Khajeh, A.; Naderi Semsani, S. Variables controlling tensile strength of stabilized sand with cement and zeolite. *J. Adhes. Sci. Technol.* **2018**, *32*, 947–962. [CrossRef]
20. Hashemi, M.; Massart, T.; Salager, S.; Herrier, G.; François, B. Pore scale characterization of lime-treated sand–bentonite mixtures. *Appl. Clay Sci.* **2015**, *111*, 50–60. [CrossRef]
21. Mola-Abasi, H.; Kordtabar, B.; Kordnaeij, A. Effect of natural zeolite and cement additive on the strength of sand. *Geotech. Geol. Eng.* **2016**, *34*, 1539–1551. [CrossRef]
22. Wei, X.; Ku, T. New design chart for geotechnical ground improvement: Characterizing cement-stabilized sand. *Acta Geotech.* **2020**, *15*, 999–1011. [CrossRef]
23. Wei, X.; Liu, H.; Ku, T. Microscale analysis to characterize effects of water content on the strength of cement-stabilized sand–clay mixtures. *Acta Geotech.* **2020**, *15*, 2905–2923. [CrossRef]
24. Jumassultan, A.; Sagidullina, N.; Kim, J.; Ku, T.; Moon, S.-W. Performance of cement-stabilized sand subjected to freeze-thaw cycles. *Geomech. Eng.* **2021**, *25*, 41–48.
25. ShahriarKian, M.; Kabiri, S.; Bayat, M. Utilization of Zeolite to Improve the Behavior of Cement-Stabilized Soil. *Int. J. Geosynth. Ground Eng.* **2021**, *7*, 35. [CrossRef]
26. Chhun, K.T.; Choo, H.; Kaothon, P.; Yune, C.Y. Experimental study on the strength behavior of cement-stabilized sand with recovered carbon black. *Geomech. Eng.* **2020**, *23*, 31–38.
27. Lu, X.L.; Yang, W.Z.; Cui, Q. Report on key technology of power transmission and transformation project under complicated geological environment. China Electric Power Research Institute, Beijing. 2014; *unpublished work*.
28. Liu, G.; Cai, M.; Huang, M. Mechanical properties of brittle rock governed by micro-geometric heterogeneity. *Comput. Geotech.* **2018**, *104*, 358–372. [CrossRef]
29. Liu, G.; Peng, J.; Zhang, Z.; Wang, Z.; Yang, Y. Numerical investigation of fluid-driven crack propagation and coalescence in granite specimen with two pre-existing flaws. *J. Nat. Gas Sci. Eng.* **2020**, *75*, 103132. [CrossRef]
30. Wang, X.; Cai, M. A comprehensive parametric study of grain-based models for rock failure process simulation. *Int. J. Rock Mech. Min. Sci.* **2019**, *115*, 60–76. [CrossRef]
31. Liu, G.; Cai, M. Modeling time-dependent deformation behavior of brittle rock using grain-based stress corrosion method. *Comput. Geotech.* **2020**, *118*, 103323. [CrossRef]
32. Cardoso, R. Influence of Water–Cement Ratio on the Hydraulic Behavior of an Artificially Cemented Sand. *Geotech. Geol. Eng.* **2017**, *35*, 1513–1527. [CrossRef]
33. Cardoso, R.; Ribeiro, D.; Néri, R. Bonding effect on the evolution with curing time of compressive and tensile strength of sand-cement mixtures. *Soils Found.* **2017**, *57*, 655–668. [CrossRef]
34. Muhammad, N.; Siddiqua, S. Stabilization of silty sand using bentonite-magnesium-alkalinization: Mechanical, physicochemical and microstructural characterization. *Appl. Clay Sci.* **2019**, *183*, 105325. [CrossRef]

Disclaimer/Publisher's Note: The statements, opinions and data contained in all publications are solely those of the individual author(s) and contributor(s) and not of MDPI and/or the editor(s). MDPI and/or the editor(s) disclaim responsibility for any injury to people or property resulting from any ideas, methods, instructions or products referred to in the content.